Establishment of a New Model Sea Anemone for Comparative Studies on Cnidarian-Algal Symbiosis

Authors: Mihirogi, Yukie, Kaneda, Michika, Yamagishi, Daisuke, Ishii, Yuu, Maruyama, Shinichiro, et al.

Source: Zoological Science, 40(3) : 235-245

Published By: Zoological Society of Japan

URL: https://doi.org/10.2108/zs220099

ZOOLOGICAL SCIENCE **40**: 235–245 (2023)

Establishment of a New Model Sea Anemone for Comparative Studies on Cnidarian-Algal Symbiosis

Yukie Mihirogi[1], Michika Kaneda[2], Daisuke Yamagishi[3], Yuu Ishii[3,4], Shinichiro Maruyama[1,3,5], Sumika Nakamura[1], Natsuno Shimoyama[2], Chihiro Oohori[1], and Masayuki Hatta[1,2*]

[1]*Department of Life Science, Graduate School of Humanities and Sciences, Ochanoizu University, Bunkyo-ku, Tokyo 112-8610, Japan*
[2]*Department of Biology, Ochanoizu University, Bunkyo-ku, Tokyo 112-8610, Japan*
[3]*Department of Ecological Developmental Adaptability Life Sciences, Graduate School of Life Sciences, Tohoku University, Aoba-ku, Sendai 980-8578, Japan*
[4]*Department of Biology, Miyagi University of Education, Aoba-ku, Sendai 980-0845, Japan*
[5]*Department of Integrated Biosciences, Graduate School of Frontier Sciences, The University of Tokyo, Kashiwanoha, Kashiwa, Chiba 277-8562, Japan*

Frequent coral bleaching has drawn attention to the mechanisms of coral dinoflagellate endosymbiosis. Owing to the difficulty of rearing corals in the laboratory, model symbiosis systems are desired. The sea anemone *Exaiptasia diaphana*, hosting clade B1 of the genus *Breviolum*, has long been studied as a model system; however, a single species is insufficient for comparative studies and thus provides only limited resources for symbiosis research, especially regarding the specificity of host-symbiont associations. We established a clonal strain of the sea anemone *Anthopleura atodai*, whose symbiont was identified as a novel subclade of *Symbiodinium* (clade A) using a novel feeding method. We also developed a method to efficiently bleach various sea anemone species using a quinoclamine-based herbicide. Bleached *A. atodai* polyps were vital and able to reproduce asexually, exhibiting no signs of harmful effects of the drug treatment. Pilot studies have suggested that host-symbiont specificity is influenced by multiple steps differently in *A. atodai* and *E. diaphana*. RNAseq analyses of *A. atodai* showed that multiple *NPC2* genes were expressed in the symbiotic state, which have been suggested to function in the transport of sterols from symbionts to host cells. These results reveal the usefulness of *A. atodai* in comparative studies of cnidarian-algal symbiosis.

Key words: *A. atodai*, *E. diaphana*, endosymbiosis, Symbiodiniaceae, model host

INTRODUCTION

Coral reef ecosystems depend on the endosymbiosis of dinoflagellates in the family Symbiodiniaceae (LaJeunesse et al., 2018) inhabiting reef-building corals, which act as primary producers through photosynthesis. However, the rise in seawater temperatures due to global warming over recent decades has led to frequent and serious bleaching of corals, threatening coral reef ecosystems. To protect and restore coral reefs, knowledge of coral-alga symbiosis mechanisms is essential for prevention of and recovery from coral bleaching (Weis, 2019). Nevertheless, there remains a lack of understanding of how symbiosis between cnidarians and algae is established, maintained, or disrupted. As the difficulty of breeding and rearing corals in the laboratory decelerates research progress, alternative model systems of host-symbionts are needed to clarify the mechanisms involved in coral-alga symbiosis.

Exaiptasia diaphana, formerly known as *Aiptasia* spp. or *Exaiptasia palida*, has been used for decades as a model animal to study cnidarian-algal symbiosis (Weis et al., 2008). *Exaiptasia diaphana* can easily be cultured in laboratory environments and can propagate even in a completely aposymbiotic state. Focusing on the specific association between host animals and algal species, heterotypic symbionts have been introduced into bleached polyps to investigate the specificity between the host and symbionts (e.g., Schoenberg and Trench, 1980; Belda-Baillie et al., 2002), and *E. diaphana* and infant polyps of *Acropora* corals show

* Corresponding author. E-mail: hatta.masayuki@ocha.ac.jp
doi:10.2108/zs220099

similar preferences for algal species during initial uptake (Hambleton et al., 2014; Wolfowicz et al., 2016). Thus, *E. diaphana* serves as a good model system for cnidarian-algal symbiosis. However, studies of only one host species may encounter difficulties in addressing questions that could potentially be solved by comparative studies of multiple host species, especially host-symbiont specificity. Host-alga specificity may be influenced by organismal activities at multiple steps in host-symbiont interactions: ingestion into the gastric cavity, endocytosis, stability of algal cells in host cells, proliferation of algal cells, exocytosis, and ejection, as schematically presented in Davy et al. (2012). Comparative studies using multiple host species are critical for specifying the steps responsible for endosymbiosis specificity in order to approach the molecular aspects involved. In this study, we sought to establish a new model of sea anemone host.

MATERIALS AND METHODS

Sea anemone culture

Polyps of *Anthopleura atodai* (Yanagi and Daly, 2004) were collected from the intertidal zone of Okinoshima Island, Tateyama, Chiba, Japan, in March 2018. The species was identified based on morphological characteristics and ITS sequences. *Exaiptasia diaphana* was collected from a culture tank at the Ooarai Aquarium in Ibaraki, Japan, in March 2017. DNA sequences of 12S rDNA matched those of *E. diaphana* (*E. pallida*) in Grajales and Rodríguez (2016). Polyps were cultured in plastic Tupperware containers with artificial seawater (ASW) (Red Sea Salt, Red Sea, Israel) in a room kept at 24–27°C and fed daily with the mashed cephalothorax part of the Argentine red shrimp *Pleoticus muelleri* available in fish markets. For each of these two anemone species, clonal strains were established by selecting individuals that exhibited high asexual reproductive activity. For experiments, an *A. atodai* clone termed TO18 and an *E. diaphana* clone OA17 were used.

Bleaching of polyps

The herbicide Kiredar (Agro-Kanesho Co., Ltd., Saitama, Japan) which is similar to herbicides such as Mogeton (Certis Biologicals, MD, USA) available in other countries, or its active ingredient, 2-amino-3-chloro-1,4 naphtoquinone (ACN) (Kanto Chemical Co., Inc., Tokyo, Japan), or quinoclamine as a common name, was dissolved in DMSO or suspended in ASW at 5 mM and added to cultures at a final concentration of 5 μM quinoclamine following preliminary investigations to identify the optimal concentration. The concentration of Kiredar was adjusted based on its 25% w/w quinoclamine content. The treatment cycle was 5-days drug exposure with continuous light exposure at approximately 1500 lx under white LED desk lights and a 2-days rest in ASW in the dark. This cycle was repeated until complete bleaching was achieved. Every 2–3 days, the pedal plane was photographed through the dish bottom using a fluorescent binocular camera (Nikon SMZ18/DS-Ri2 CCD camera), and the intensity of red fluorescence was evaluated using ImageJ. Ejected algal cells during and after the bleaching treatment were observed using a fluorescence microscope (Olympus FSX100).

Inoculation of algal cells into bleached polyps

The species and subclades of the symbiont algae and their hosts are listed in Table 1. Subclades were identified based on ITS sequences. In this study, symbiont algae are indicated by subclades to facilitate comparison with previous literature. Algal cells were collected from the host anemone species for each algal species by mashing host tentacle tissues in ASW. Subclade A3 was obtained by introducing algae from the giant clam *Tridacna crocea*, which hosts both A3 and C1, into newly formed spats of the coral *Acropora tenuis*, which incorporates A3 but not C1 at this stage (Yorifuji et al., 2017). Specific incorporation of A3 was confirmed by DNA analyses. Subclade A25 was used immediately after prepara-

Table 1. Algal species, ITS accession number (acc. no.), host origin, and average diameter of algal cells (n = 20).

Species	subclade	acc. no.	host	collection location	average±SD (μm)
Symbiodinium sp.	A25	LC718587	*Anthopleura atodai*	Tateyama, Chiba	8.9 ± 0.86
Breviolum minutum	B1	LC718588	*Exaiptasia diaphana*	Ooarai Aquarium	7.9 ± 0.73
Symbiodinium tridacnidorum	A3	LC718591	*Tridacna crocea*	Naha market, Okinawa	9.6 ± 1.17
Cladocopium goreaui	C1	LC718589	*Mesactinia ganensis*	Marine St., Univ. Ryukyu	10.3 ± 1.37
Durusdinium trenchii	D1a	LC718590	*Amphiactis orientalis*	Sesoko Island, Okinawa	10.2 ± 1.03
Fugacium sp.	F7	LC718592	*Anthopleura uchidai*	Tateyama, Chiba	8.7 ± 0.69

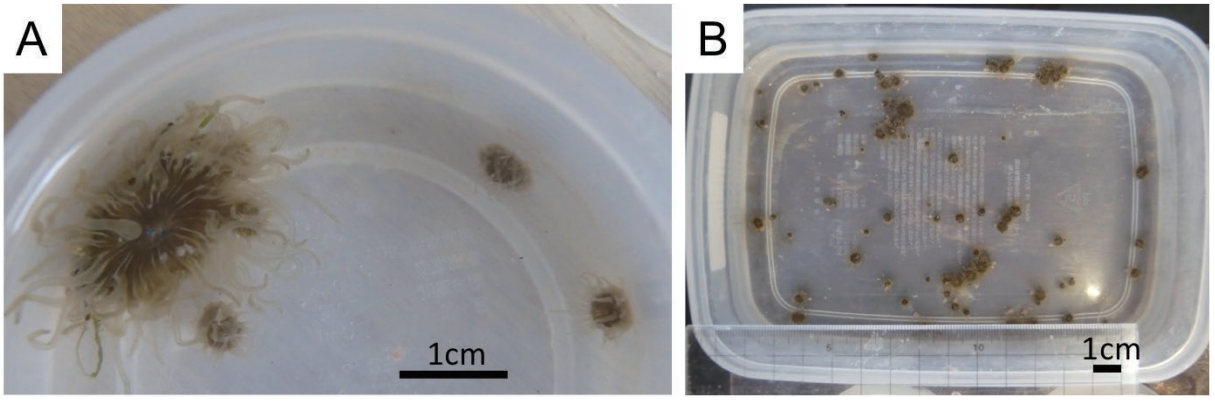

Fig. 1. Clonal culture of *A. atodai*. **(A)** Five small polyps were produced 2 months after collection in clonal culture. **(B)** Approximately 60 polyps were produced from a single polyp by asexual production after 9 months.

tion because this species died in seawater within the day after isolation from host tissues. The other species were used the day after preparation to allow flagellum formation. Each bleached polyp was placed in a well of a 6-well multidish with 5 mL of ASW, and algal cells were added to a density of 5×10^5 cells/mL and washed away after incubation for 5 h with swirling of water at 30 rpm using a handmade mixing apparatus (see Supplementary Figure S1). The ASW was changed every day without feeding. Fluorescent beads (Fluoresbrite Plain Microspheres 6.0 μm YG, Polysciences, PA, USA) were administered at 1000 particles/mL.

Identification of algal subclades

DNA was extracted from host tissues according to Sargent et al. (1986). PCR for algal genotyping was performed with a Symbiodiniaceae-specific primer set: 5′-CCGGTGAATTATTCGGACTGACGCAGTGCT-3′ for the forward primer and 5′-TCCTCCGCTTATTGATATGC-3′ for the reverse primer. For typing of *E. diaphana*, 12S rDNA was amplified using the primer set 5′-CCGGTGAATTATTCGGACTGACGCAGTGCT-3′ and 5′-TCCTCCGCTTATTGATGC-3′ (Lauretta et al., 2014), For typing of *A. atodai*, a primer set targeting nuclear ITS, 5′-AGGTGAACCTGCGGAAGGATCA-3′ (Apakupakul et al., 1999) and 5′-CTGTTCCGCAACTTGGAC-3′, was used for amplification. PCR products were purified using the GENECLEAN II kit (MP Biomedicals, CA, USA) and sequenced using an ABI BigDye v3.1 Cycle Sequencing Kit and a 3730x DNA sequencer. The full-length ITS sequences were subjected to phylogenetic analyses using MEGA7 (Kumar et al., 2016). After aligning of sequences by Muscle, alignments were corrected by hand. Neighbor-joining was used to construct phylogenetic trees.

RNA extraction and reference transcriptome sequencing

One symbiotic and one apo-symbiotic *A. atodai* used for RNA extraction were cultured under LED light irradiation (7 μmol $s^{-1}m^{-2}$) with an 18 h light:6 h dark cycle and 24 h dark conditions, respectively, in ASW (Instant Ocean Sea Salt, Instant Ocean, VA, USA) at 20°C. Each sample was placed in a microtube with RNAlater RNA Stabilization Solution (ThermoFisher Scientific, MA, USA) for 1–2 hours, blotted with Kimwipes tissue paper, and then placed into a mixture of 8 μL thioglycerol and 400 μL homogenization buffer. The samples in the thioglycerol and homogenization mixture were ground with a Biomasher II (Nippi, Tokyo, Japan) until pieces of tissue were no longer observed. After standing for 10 min, the mixtures were centrifuged for 2 minutes at 12,000 × *g* and the supernatants were used for RNA extraction using the Maxwell RSC Plant RNA Kit (Promega Corporation, WI, USA) according to the manufacturer's instructions. The quality and quantity of the extracted RNA were measured using an Agilent RNA 6000 Nano Kit on an Agilent Bioanalyzer (Agilent Technologies, CA, USA) and a NanoDrop spectrophotometer (Thermo Fisher Scientific, MA, USA), respectively. Non-directional library preparation and RNA-seq were outsourced to Filgen (Aichi, Japan). Sequencing was performed using an Illumina NovaSeq6000 instrument (paired-end, 150 bp). The raw read data are available from the DDBJ/EMBL/GenBank database under BioProject accession number PRJDB14295.

Sequence assembly and phylogenetic tree construction

All DNA sequencing reads of the two samples (33,609,878 and 34,973,663 reads for symbiotic and apo-symbiotic samples, respectively) were assembled into contigs using the Trinity program (v.2.11.0) (Grabherret et al., 2011) using a '--trimmomatic' option. The longest open reading frames of the assembled contigs with functional gene annotations were predicted using TransDecoder (v.5.5.0) with a '--single_best_only' option (Haas et al., manuscript in prep. http://transdecoder.github.io). The *A. atodai NPC2* gene was translated into protein. The NPC2 protein sequences of other animal species used for constructing an NPC2 phylogenetic tree were obtained from sequences used in a previous study (Ishii et al., 2019). All NPC2 protein sequences were aligned using MAFFT v.7.490 (Katoh et al., 2013) with '--localpair --maxiterate 1000' options. The alignment was trimmed using TrimAl (v.1.4.1) (Capella-Gutiérrez et al., 2009) using the '-gt 0.8' option, and used for construction of a maximum likelihood tree using IQ-TREE (v.2.1.2) with the WAG + I + G4 model selected using the ModelFinder program in IQ-TREE (Nguyen et al., 2015; Kalyaanamoorthy et al., 2017).

RESULTS

Clonal culture of *A. atodai*

In addition to morphological identification, ITS sequences matched the registered data (accession no. KT852185) for *A. atodai* (Larson and Daly, 2016). *Anthopleura atodai* asexually brooded and expelled small polyps as described by Yanagi and Daly (2004). The founder polyp of *A. atodai* reproduced approximately 60 new polyps during 9 months of culture (Fig. 1), corresponding to more than one polyp per week under culture conditions. Subsequently, as a population including immature polyps, 20 polyps produced 144 new polyps in 45 days, 0.16 polyps per individual per day on average. Feeding with mashed shrimp was empirically found to promote efficient growth of the anemone compared to *Artemia nauplii*. Daily feeding may promote asexual

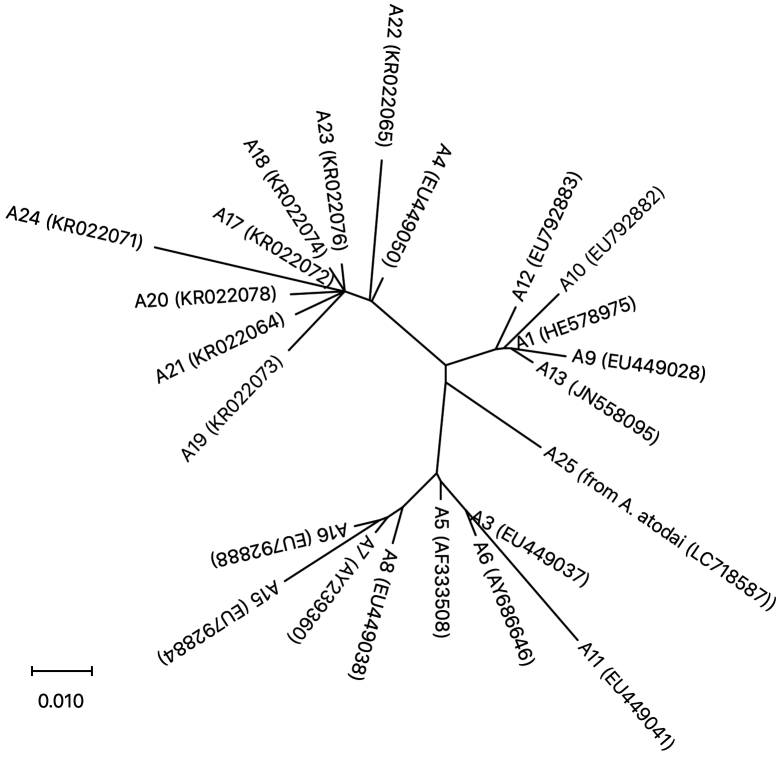

Fig. 2. ITS phylogeny of *Symbiodinium* (clade A) and the symbiont alga in *A. atodai*.

reproduction, as it reduces the polyp size from 1 cm at capture to 5 mm in diameter after prolonged culture. Newborn polyps took 3 months to grow to 3 mm in diameter, which is a suitable size for experiments, and more than half a year until maturation for asexual reproduction. Sexual traits were not investigated, but there were no signs of sexual reproduction under our culture conditions.

Identification of symbiont algae in *A. atodai* and other donor hosts

BLAST results using the obtained ITS sequence of the algae hosted by *A. atodai* revealed high similarity to sequences suggesting that *A. atodai* hosts algae in the genus *Symbiodinium* (clade A). Sequence data containing subclade annotations were collected from DDBJ/GenBank and subjected to multiple alignments. Phylogenetic analyses using the neighbor-joining method revealed that this algal sequence corresponded to a novel subclade in the *Symbiodinium* clade (clade A) (Fig. 2). We designated this novel subclade A25 in this study. The algal sequence obtained from a polyp of *Anthopleura uchidai* also constituted a novel subclade in the genus *Fugacium* (clade F) and is dealt with as F7. Since *A. uchidai* is known to be polymorphic in symbiosis with algae of clades F and A (Miura et al., 2014), we used subclade F7 algae taken from a single polyp. The other algae in Table 1 matched the registered sequences with the subclade annotations. The diameters of the algal cells were measured and are shown in Table 1. The sizes of the algae differed slightly, ranging from approximately 8–10 μm in diameter.

Bleaching of sea anemones using quinoclamine

After trials for determining drug concentrations and light durations for effective bleaching, we identified a suitable condition composed of repeated cycles of 5-days of drug exposure at 5 μM quinoclamine under continuous light followed by 2-days of rest without the drug in the dark. For use of the herbicide Kiredar, the concentration was adjusted to contain 5 μM of the active ingredient quinoclamine. Figure 3 presents the changes in red fluorescence intensity by tracing each single polyp treated in a well of a 6-well multidish. The patterns of fluorescence decrease were similar between polyps

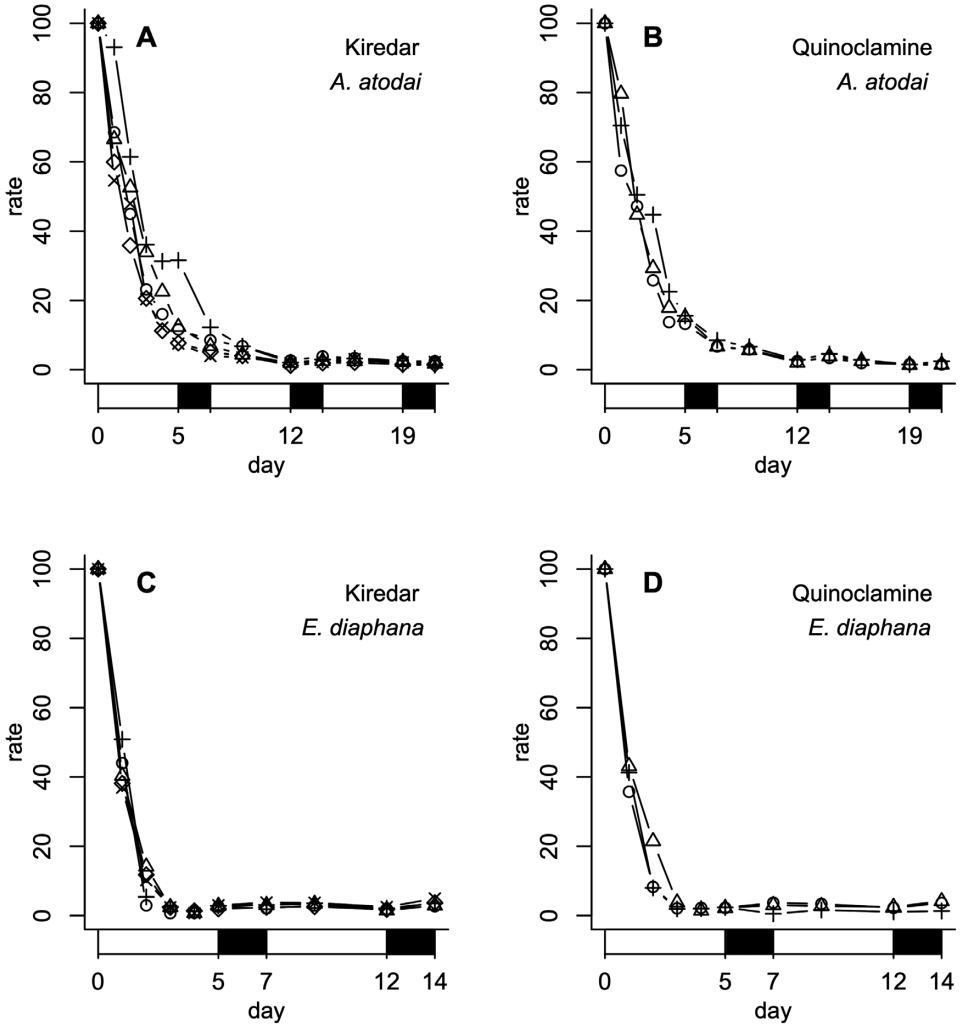

Fig. 3. Relative intensity of chlorophyll red fluorescence on the pedal plane. Intensity was evaluated for each individual polyp comparing to day 0 value as 100%. **(A)** *A. atodai* treated with Kiredar (n = 5). **(B)** *A. atodai* treated with pure quinoclamine (n = 5). **(C)** *E. diaphana* treated with Kiredar (n = 3). **(D)** *E. diaphana* treated with pure quinoclamine (n = 3). Dark rest periods are shown by shadows.

treated with Kiredar and pure quinoclamine. Red fluorescence of algae at the pedal disc decreased to less than 20% during the first 5 days of exposure in *A. atodai* and less than 10% in 2 days in *E. diaphana*. Fluorescence intensity at the pedal dropped below the detection level after two cycles of treatment in *A. atodai* and after one cycle in *E. diaphana*, whereas small numbers of algae remained in the tentacles and body column. *Anthopleura atodai* maintained no red fluorescence of algae after three cycles of treatment, and *E. diaphana* after two cycles (Fig. 4). Complete bleaching was confirmed by observing no recovery of algae in the bleached polyps after normal culture for more than 2 weeks. Exposure to 5 μM quinoclamine for 5 days in the dark caused no obvious decrease in the red fluorescence of algae in *A. atodai*, suggesting that photochemical reactions caused bleaching. Bleached polyps were reared with feeding for more than 2 years, and asexual reproduction was observed as in wild-type symbiotic polyps. Kiredar treatment was efficient for bleaching other sea anemone species; *Anthopleura uchidai* (Fig. 5), and *Mesactinia ganensis* (data not shown). A bleached polyp of *A. uchidai* spawned eggs 8 months after bleaching with Kiredar treatment.

Algal cells ejected from hosts during Kiredar treatment under continuous light for 16 h were observed using light and fluorescence microscopy. Algal cells are distinguished from host cells and debris by their round shape and size. Almost all ejected algal cells retained a brown color. Red fluorescence of chlorophyll was not reduced in algae ejected by *A. atodai* or *E. diaphana* after treatment in comparison with freshly prepared algae, but was reduced in algae ejected by a polyp of *A. uchidai* hosting clade A (see Supplementary Figure S2).

Pilot comparative experiments on host-symbiont specificity

Ingestion step: Two weeks after complete bleaching, the absence of algae in polyps was confirmed by fluorescent binocular observations, and bleached polyps were used for the re-introduction of algae. For each batch, five bleached polyps were exposed to algae for 5 h, swirling in a well of a 6-well multidish. The presence of algae inside the hosts was observed 7 d after inoculation (Table 2). At 100 cells/mL of algal cells, *A. atodai* did not incorporate any of the six algal species, including the native symbiont A25, whereas *E. diaphana* incorporated B1 and A3. *Anthopleura atodai* did not take up any algae even at 10,000 cells/mL, which is an extremely high density compared to natural situations. On the other hand, *E. diaphana* took up C1, D1a, and F7 at high

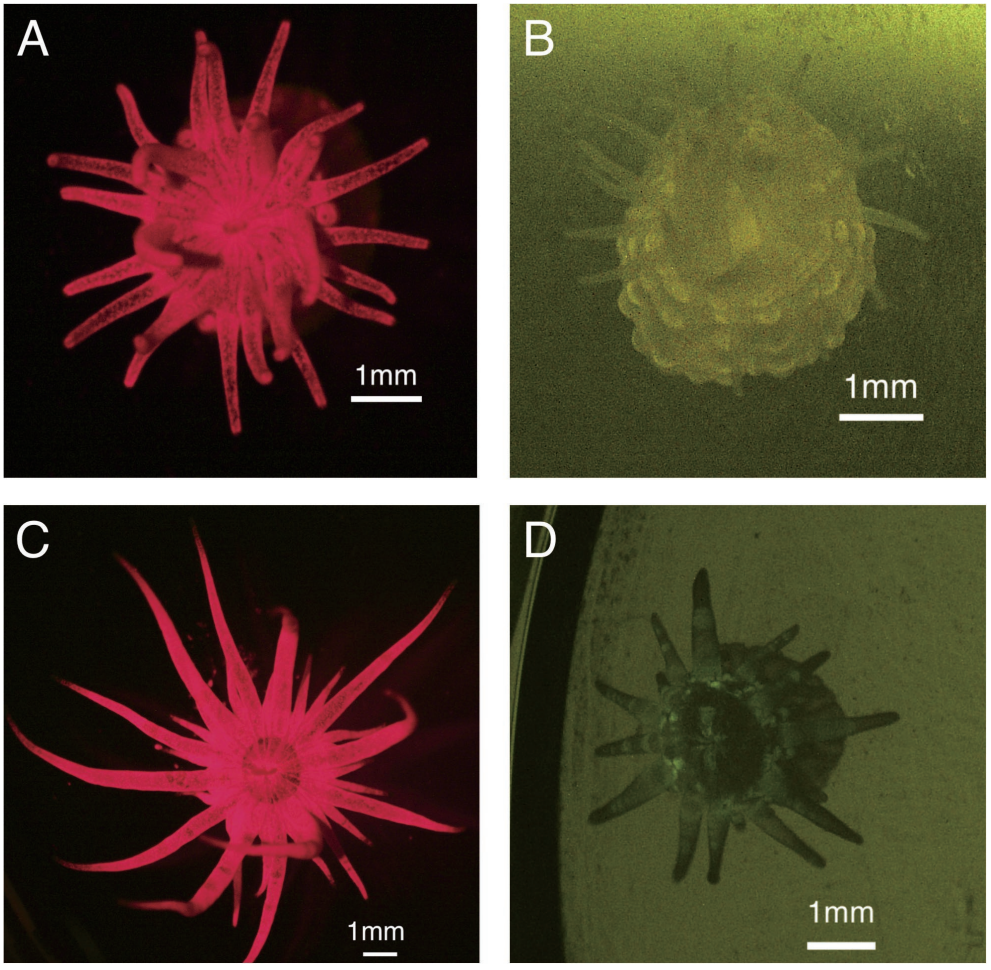

Fig. 4. Fluorescent photographs of wild and bleached polyps. **(A)** Wild-type *A. atodai*. **(B)** Bleached *A. atodai*. **(C)** Wild-type *E. diaphana*. **(D)** Bleached *E. diaphana*.

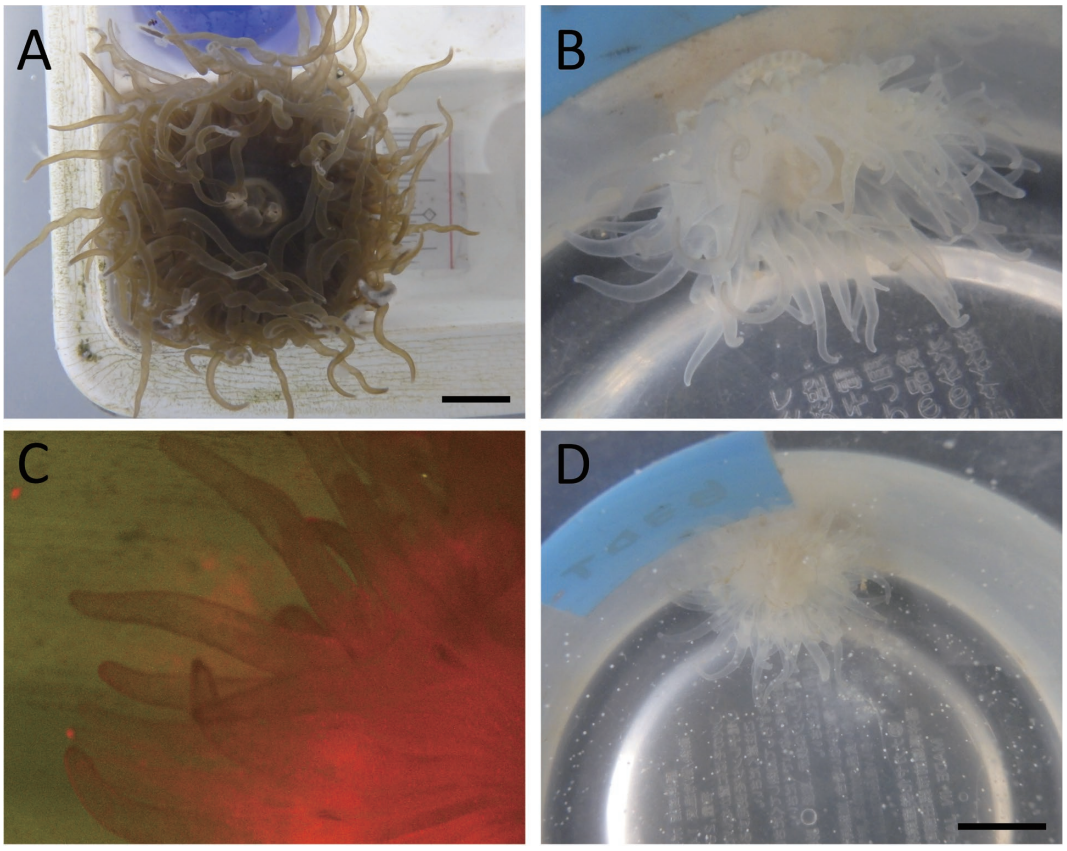

Fig. 5. *A. uchidai* bleached using the herbicide Kiredar at 5 μM effective quinoclamine concentration for 2 weeks. **(A)** An untreated polyp. **(B)** A bleached polyp 8 months after bleaching. **(C)** Fluorescent microscopy revealing absence of algae after Kiredar treatment. **(D)** Spawning of eggs by a bleached polyp 8 months after bleaching. Scale bar = 1 cm.

Table 2. Ingestion specificity under different inoculation conditions. Five polyps were used for each experimental batch, and fluorescence was observed 7 days after inoculation. Numbers of polyps which incorporated algae are shown.

algal cell density	A25	B1	A3	C1	D1a	F7
A. atodai						
100/mL	0	0	0	0	0	0
10,000/mL	0	0	0	0	0	0
10,000/mL + food	5	5	4	5	4	5
E. diaphana						
100/mL	0	5	5	0	0	0
10,000/mL	0	–	–	4	5	2
10,000/mL + food	0	–	–	–	–	4

density. When an aliquot (20 μL) of mashed shrimp was dispersed together with algae at 10,000 cells/mL in each well, *A. atodai* incorporated all of the algal species. Clade A25 was not taken up by *E. diaphana*, even when applied with food.

Propagation step: Polyps that incorporated algal cells were observed to show changes in algal cell numbers for individual polyps until 21 d after inoculation (Fig. 6). Although accurate numbers could not be counted and the results varied by individual, approximate tendencies of algal cell propagation were distinguished between different combinations of hosts and algae. A25 numbers increased very slowly in the native host *A. atodai*, but did not increase in *E. diaphana*. B1 increased slowly in *A. atodai*, but faster than its native symbiont A25, and quickly propagated in its native host, *E. diaphana*. A3 revealed patterns similar to those observed for B1. C1 increased to and remained at low densities in both host anemones. D1a showed similar patterns to C1 in *A. atodai* but varied by individual hosts from an increase to a decrease in *E. diaphana*. F7 increased once and decreased gradually in *A. atodai*, but only decreased in *E. diaphana*. After long-term culture for more than 2 months of polyps inoculated with heterologous symbionts, *A. atodai* harbored B1 at high densities and C1 at low densities (Fig. 7). A3 showed rapid propagation in the initial phase (Fig. 6) but resulted in low densities in the stable phase in *E. diaphana* (Fig. 7).

Ejection step: To compare the ejection speeds of nonspecific particles after incorporation, fluorescent plastic beads were mixed with food and fed, and their numbers were traced. Although the speed of the decrease varied among individuals, incorporated beads disappeared in several days, and obvious differences were not observed between the two anemone species (Fig. 8).

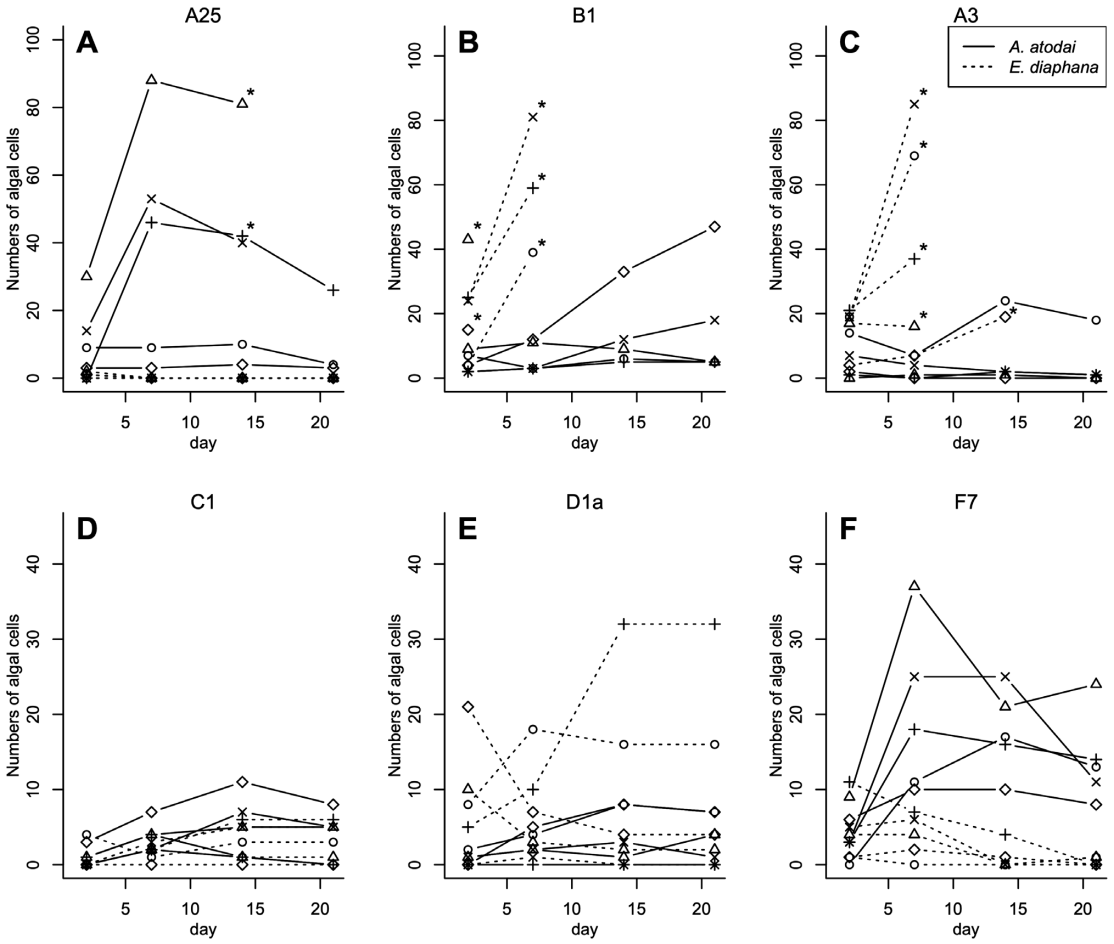

Fig. 6. Propagation of symbiont algae after inoculation into bleached polyps. The vertical axis represents numbers of algae observed in the tentacles and oral disc, and the horizontal axis represents days after introduction of algae. The solid lines represent *A. atodai* and the dashed lines represent *E. diaphana* for each polyp. Plots are not shown when the numbers of algae became too great to count. Note that the scale of vertical axes in upper panels is approximately twice that of lower panels.

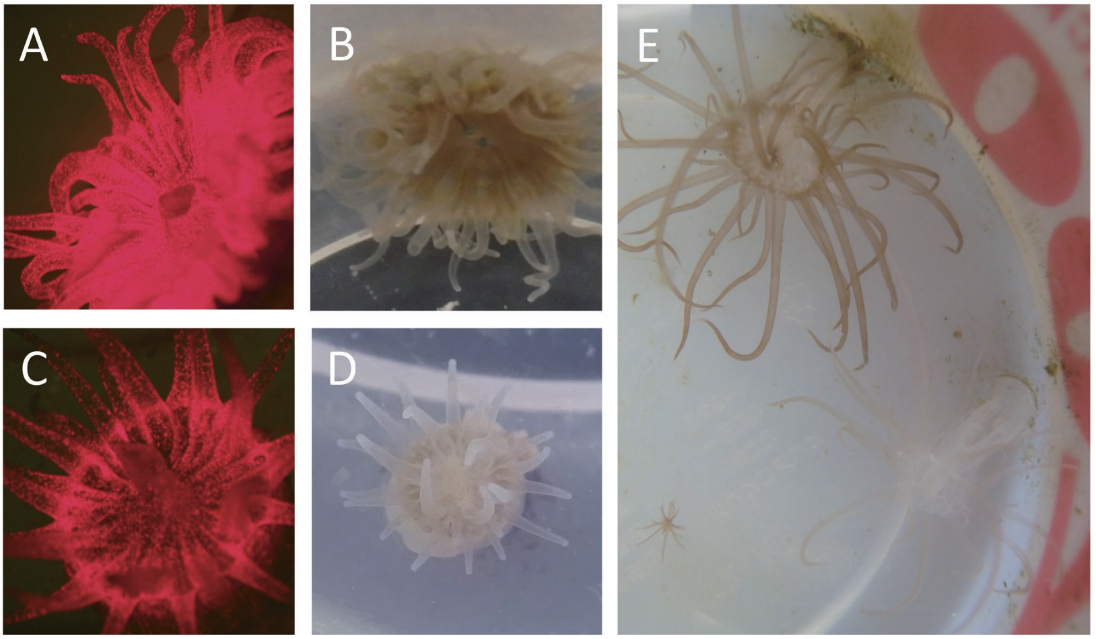

Fig. 7. Long-term culture of polyps inoculated with heterologous symbionts. **(A)** 2 months and **(B)** 1 year after inoculation of clade B1 into *A. atodai*. **(C)** 2 months and **(D)** 1 year after inoculation of clade C1 into *A. atodai*. **(E)** 3 months after inoculation of clade A3 into *E. diaphana*.

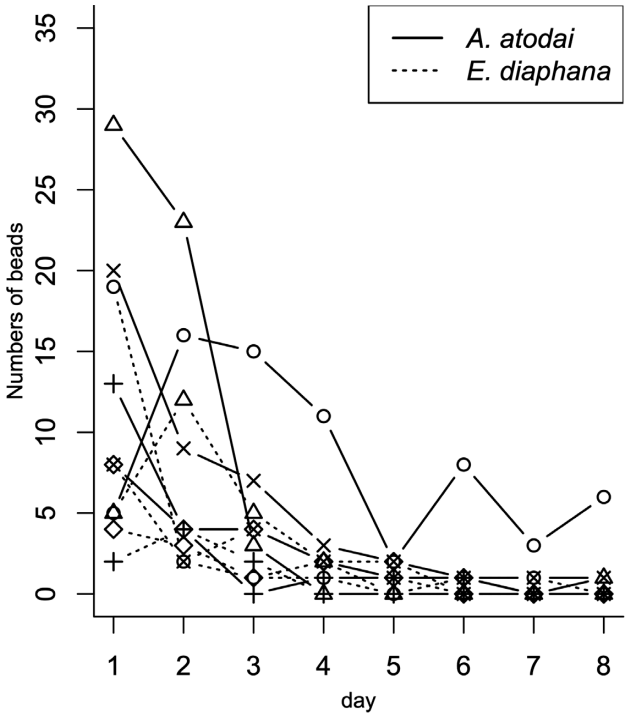

Fig. 8. Decrease of fluorescent beads once incorporated into the oral disc and tentacles. The solid lines represent *A. atodai* and the dashed lines represent *E. diaphana* for each polyp (n = 5). The vertical axis represents numbers of beads observed in one individual polyp, and the horizontal axis represents days after introduction of beads.

Reference transcriptome of *A. atodai*

To facilitate gene-level analyses of the new model sea anemone, reference transcriptome data were generated using a symbiotic and bleached (apo-symbiotic) individual. Similarity searches identified symbiosis-related genes, including those encoding the conserved sterol transporter Niemann-Pick Type C2 (NPC2) (Dani et al., 2014; Hambleton et al., 2019). Phylogenetic analysis of NPC2 protein sequences showed that *A. atodai* expressed multiple isoforms, forming clusters corresponding to one canonical and three non-canonical variants of the *NPC2* gene, each of which was closely related to the counterpart found in *Anemonia viridis* (Fig. 9).

DISCUSSION

Establishment of a clonal strain of *A. atodai* as a new model system

Here, we established a clonal strain of the sea anemone *A. atodai*. This strain produced an average of 0.16 polyps per individual per day by asexual reproduction in the laboratory environment. This propagation rate meets the requirements of most molecular and cellular biological experiments. In addition, bleached polyps are capable of asexual propagation. The improvement of food supply methods is critical to achieve successful culture of *A. atodai*. Mashed shrimp as feed enabled stable maintenance and propagation of not only *A. atodai*, but also several other species in which long-term culture in the laboratory was difficult by feeding with *Artemia nauplii*. Tiny polyps can also be cultured by suspending mashed shrimp in culture water, enabling the culturing of tiny polyps and physiological experiments using various anemone species.

An alternative focus is the evolution of endosymbiosis within the genus *Anthopleura*. In the rocky intertidal zone of middle Japan, there are several sympatric species, such as *A. atodai*, *A. asiatica*, *A. inornata*, *and A. uchidai* hosting different species of Symbiodiniaceae, and *A. pacifica* and *A. fuscoviridis* being aposymbiotic. In addition to molecular phylogenetic analyses, comparative experiments regarding host-symbiont specificities and physiological responses will support the elucidation of evolutionary histories of host *Anthopleura* and symbiont lineages involving the establishment of their mutual association in the temperate coast of Japan. The establishment of methods for the long-term culture and bleaching of various anemone species in this study will provide opportunities for comparative studies surrounding anemone-alga endosymbiosis.

Bleaching of sea anemones by quinoclamine

Quinoclamine is phototoxic to algae and liverworts. This study showed that it also acts on the removal of dinoflagellate algae of Symbiodiniaceae from sea anemone hosts. As the bleaching pace did not differ between Kiredar and quinoclamine exposure (Fig. 3), the observed bleaching is thought to be due to the action of quinoclamine. Quinoclamine has been shown to inhibit chlorophyll synthesis (Koura et al., 1994), but mechanisms of phototoxicity have not been clarified. Even if chlorophyll synthesis can be inhibited by Kiredar treatment in some cases, it is likely that such inhibition was not a major cause of ejecting algal cells, considering the lack of obvious reduction in algal cells ejected by *A. atodai* (see Supplementary Figure S2). Based on the structural features of quinones, it is presumed that quinoclamine removes electrons from the photosystem (Altland et al., 2011), like the herbicide paraquat (Qian et al., 2009), and results in the generation of reactive oxygen species (ROS), which is suggested to be a major cause of bleaching in corals (Lesser, 2011). This also seems to be the case in sea anemone bleaching, considering our findings that bleaching occurred under light, but not dark, conditions.

Although the property elicited by the action of quinoclamine as the cause of algal cell ejection remains to be clarified, this drug is efficient in eliminating Symbiodiniaceae algae from sea anemone hosts without irreversible harm if treated appropriately, as shown by rearing for long periods accompanied by asexual reproduction. Menthol (Matthews et al., 2016) and 3-(3,4-dichlorophenyl)-1,1-dimethylurea (DCMU) used for the herbicide diuron (e.g., Xiang et al., 2013) and heat treatment (e.g., Belda-Baillie et al., 2002) have been utilized to bleach *Exaiptasia*. However, this study revealed the efficiency of quinoclamine, which is commercially available as a cheap herbicide, as an alternative bleaching tool for the bleaching of a variety of sea anemone species, such as *A. uchidai* (Fig. 6) and *M. ganensis*, which died before bleaching by heat treatment (data not shown), in addition to *A. atodai* and *E. diaphana* (Figs. 4, 5).

Pilot experiments of comparative studies on symbiotic specificity

To assess the suitability of *A. atodai* for comparative

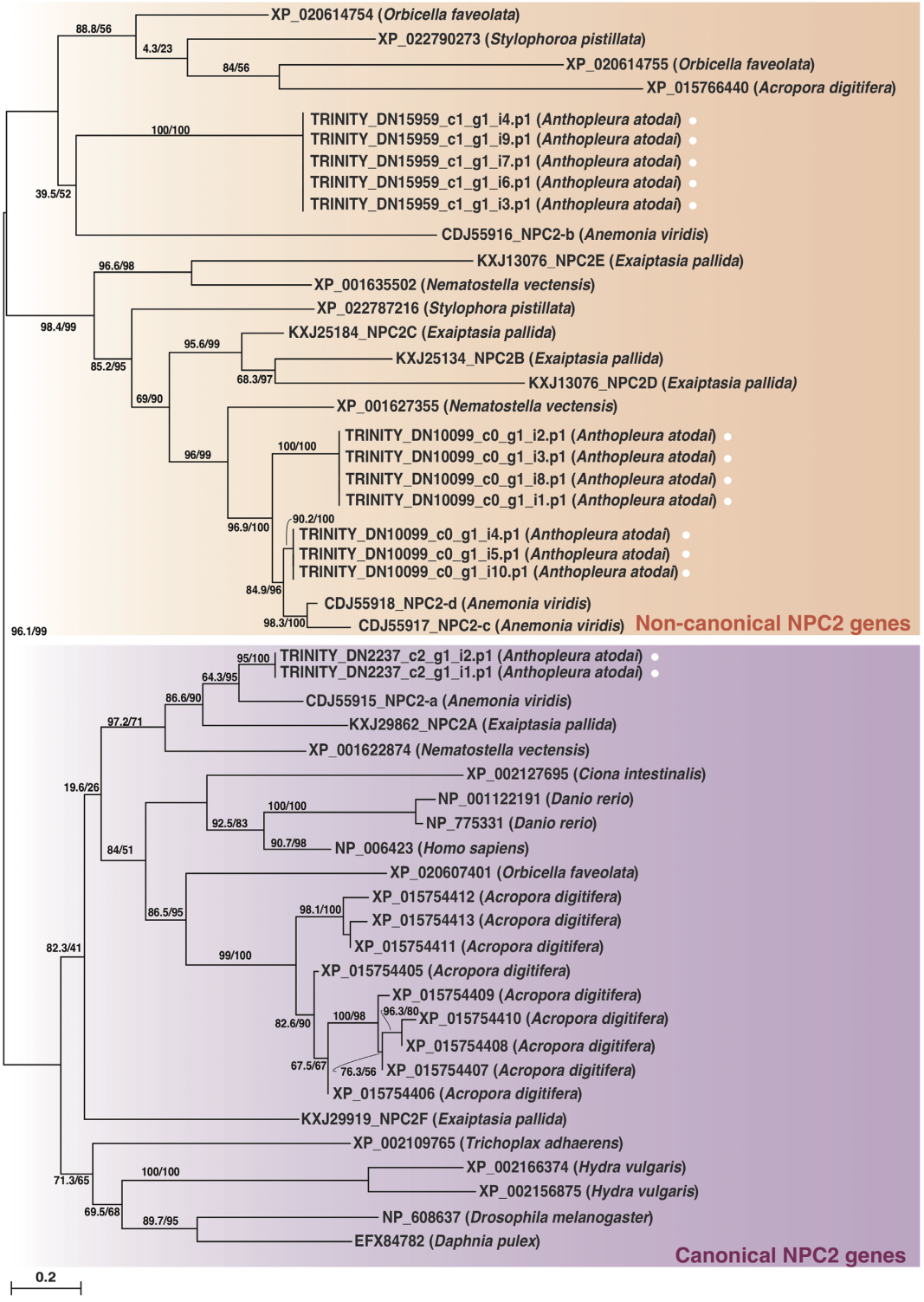

Fig. 9. A phylogenetic tree of NPC2 proteins. White circles indicate NPC2 isoforms identified in this study.

studies on host-symbiont specificity, small-scale pilot experiments were conducted.

Specificity at the ingestion step differed between *A. atodai* and *E. diaphana* (Table 2). *Anthopleura atodai* ingested algal cells only when the algae were applied together with food, even when they were native symbionts. These results suggested that foods simply stimulate ingestion activity without masking the surface molecules responsible for recognition of algae. Similar stimulation of algal cell ingestion by adding food was observed in larvae of the coral *Fungia scutraia* (Schwartz et al., 1999). In contrast, *E. diaphana* incorporated five algal species without food, revealing a high ingestion activity. The lack of uptake of A25 by *E. diaphana* can be explained by positive rejection. Algal

cell size is unlikely to influence ingestion efficiency because the size range of all algal cells tested in this study was approximately 8–10 μm (Table 1), which was shown to be acceptable for *Exaiptasia* (*Aiptasia*) (Biquand et al., 2017). Specific molecules on the algal cell surface may affect ingestion efficiency. In case of the coral *Acropora*, favored clades were incorporated at low density (1 algal cell/mL, Yamashita et al., 2014), on the other hand, unfavored clades were not even at high density (10,000 algal cells/mL, Wolfowicz et al., 2016). Future studies will be conducted to screen untested clades seeking those rejected by the sea anemones and to clarify the molecular mechanisms of algal cell selection at the ingestion step and to examine whether attractive or repellent molecules are presented by algae and the receptor molecules expressed in the host mouth.

Specificity at the propagation step also differed between the two host species (Fig. 5). Algal cell propagation was slow in *A. atodai*, except in F7, which increased once and then decreased. In *A. atodai*, even its native symbiont A25 increased slowly, in contrast to the rapid propagation of B1 in *E. diaphana*. *Exaiptasia diaphana* allowed swift propagation of A3, but no propagation of F7. The propagation speed may be a result of a balance between the proliferation rate and decreasing speed of algal cells. The decreasing speed can be divided into the speeds of intracellular digestion, exocytosis, and ejection from the host mouth. Quantifying the speed of each process is also a challenge for future studies. We tried to compare the ejection steps using plastic beads, but no obvious differences were detected (Fig. 7). Considering the observation that ejected algal cells were often found at the bottom of *E. diaphana* culture ware, *E. diaphana* seems to eject excessive algal cells produced by high-speed growth. However, ejected algal cells were less abundant in *A. atodai* cultures. In addition to differences in proliferation speed, there may be different ejection speeds specific to algal species in each host, even if differences were not detected in the ejection speed of plastic beads. Digestion of algal cells by host cells is thought to be another possible reason for the decrease in algal cells, especially in *A. atodai*.

Another aspect of interest is the regulation of algal cell densities in the steady state in the host body, which should also be determined by the balance between proliferation and decrease. Preliminary long-term observations revealed a lower density of algae in some heterologous combinations of host and algal species than in native combinations (Fig. 7; Medrano et al., 2019). The rate of algal cell proliferation and decrease might change from the initial phase of inoculation to the stable phase depending on algal cell densities in the host body and host responses to algae. Specificity at each step concerning the initiation and maintenance of endosymbiosis must be examined in order to understand the total specificity of cnidarian-algal association in dynamic equilibrium. Comparative studies using multiple host-symbiont systems will help to dissect the complex of multiple steps responsible for endosymbiosis and to choose approaches for the identification of molecular mechanisms by focusing on each step.

We present a reference transcriptome analysis to support molecular-level studies in *A. atodai*. For instance, *A. atodai* expresses a repertoire of genes encoding multiple NPC2 variants (Fig. 9), which are known to be important for the transport of sterols from symbiotic algal cells to host cells, thus providing a basis for comparative molecular studies on endosymbiosis using current (Dani et al., 2014; Hambleton et al., 2019) and new model cnidarian species. Future comparative omics studies concerning heterologous host-symbiont combinations, with a focus on these symbiosis-related genes, will shed light on the molecular aspects of each step of endosymbiosis that determine host-symbiont specificity, and these studies are now ready to be launched.

CONCLUSION

A clonal strain of the sea anemone *A. atodai* was established as a new model system for cnidarian-algal endosymbiosis by establishing new culture and bleaching methods. Pilot experiments suggested that algal cell ingestion and propagation steps were differently involved in host-symbiont specificity in *A. atodai* and *E. diaphana*. Our study demonstrates the suitability of this new strain of *A. atodai* for comparative studies surrounding host-symbiont specificity.

ACKNOWLEDGMENTS

We thank Mr. Yojiro Shiba at Ooarai Aquarium for providing *E. diaphana* polyps, and Dr. Kensuke Yanagi for species identification of *M. ganensis* and notation of *A. uchidai*. Computations were partially performed on the NIG supercomputer at ROIS National Institute of Genetics.

AUTHOR CONTRIBUTIONS

YM, MK, NS, SN, CO, MH performed wet experiments. DY, YI, SM did RNAseq. YM, SM, MH drafted the primary manuscript.

SUPPLEMENTARY MATERIALS

Supplementary materials for this article are available online. (URL: https://doi.org/10.2108/zs220099)

Supplementary Figure S1. Mixing apparatus.

Supplementary Figure S2. Color and fluorescence of ejected algal cells during bleaching treatment.

REFERENCES

Altland JE, Wehtje G, Sibley J, Miller M, Gilliam C, Krause CR (2011) Differential response of liverwort (*Marchantia polymorpha*) tissue to POST-applied quinoclamine. Weed Technol 25: 580–585

Belda-Baillie CA, Baillie BK, Maruyama T (2002) Specificity of a model cnidarian-dinoflagellate symbiosis. Biol Bull 202: 74–85

Biquand E, Okubo N, Aihara Y, Rolland V, Hayward DC, Hatta M, et al. (2017) Acceptable symbiont cell size differs among cnidarian species and may limit symbiont diversity. ISME J 11: 1702–1712

Capella-Gutiérrez S, Silla-Martínez JM, Gabaldón T (2009) trimAl: a tool for automated alignment trimming in large-scale phylogenetic analyses. Bioinformatics 25: 1972–1973

Dani V, Ganot P, Priouzeau F, Furla P, Sabourault C (2014) Are Niemann-Pick type C proteins key players in cnidarian-dinoflagellate endosymbioses? Mol Ecol 23: 4527–4540

Davy SK, Allemand D, Weis VM (2012) Cell biology of cnidarian-dinoflagellate symbiosis. Microbiol Mol Biol Rev 76: 229–261

Grabherret MG, Haas BJ, Yassour M, Levin JZ, Thompson DA, Amit I, et al. (2011) Full-length transcriptome assembly from RNA-Seq data without a reference genome. Nat Biotechnol 29: 644–652

Grajales A, Rodríguez E (2014) Morphological revision of the genus *Aiptasia* and the family Aiptasiidae (Cnidaria, Actiniaria, Metridioidea). Zootaxa 3826: 55–100

Grajales A, Rodríguez E (2016) Elucidating the evolutionary relationships of the Aiptasiidae, a widespread cnidarian–dinoflagellate model system (Cnidaria: Anthozoa: Actiniaria: Metridioidea). Molecular Phylogenet Evol 94: 252–263

Hambleton EA, Jones VA, Maegele I, Kvaskoff D, Sachsenheimer T, Guse A (2019) Sterol transfer by atypical cholesterol-binding NPC2 proteins in coral-algal symbiosis. eLife 8: e43923

Ishii Y, Maruyama S, Takahashi H, Aihara Y, Yamaguchi T, Yamaguchi K, et al. (2019) Global shifts in gene expression profiles accompanied with environmental changes in cnidarian-dinoflagellate endosymbiosis. G3: Genes Genomes|Genet 9: 2337–2347

Kalyaanamoorthy S, Minh BQ, Wong TKF, von Haeseler A, Jermiin LS (2017) ModelFinder: fast model selection for accurate phylogenetic estimates. Nat Methods 14: 587–589

Kato K, Standley DM (2013) MAFFT Multiple Sequence Alignment Software Version 7: Improvements in Performance and Usability. Mol Biol Evol 30: 772–780

Koura S, Takasuka K, Katsuyama N, Ogino C, Sato Y, Wakabayashi K (1994) Mode for herbicidal action of 2-Amino-3-chloro-1,4-naphthoquinone (ACN). Biosci Biotech Biochem 58: 1210–1212

Kumar S, Stecher G, Tamura K (2016) MEGA7: Molecular evolutionary genetics analysis version 7.0 for bigger datasets. Mol Biol Evol 33: 1870–1874

LaJeunesse TC, Parkinson JE, Gabrielson PW, Jeong HJ, Reimer JD, Voolstra CR, Santos SR (2018) Systematic revision of Symbiodiniaceae highlights the antiquity and diversity of coral endosymbionts. Curr Biol 28: 2570–2580

Larson PG, Daly M (2016) Phylogenetic analysis reveals an evolutionary transition from internal to external brooding in *Epiactis* Verrill (Cnidaria: Anthozoa: Actiniaria) and rejects the validity of the genus *Cnidopus* Carlgren. Mol Phylogenet Evol 94: 548–558

Lesser MP (2011) Coral bleaching: causes and mechanisms. In: "Coral Reefs: An Ecosystem in Transition" Ed by Z Dubinsky, N Stambler, Springer, Dordrecht, pp 405–419

Matthews JL, Sproles AE, Oakley CA, Grossman AR, Weis VM, Davy SK (2016) Menthol-induced bleaching rapidly and effectively provides experimental aposymbiotic sea anemones (*Aiptasia* sp.) for symbiosis investigations. J Exp Biol 219: 306–310

Medrano E, Merselis DG, Bellantuono AJ, Rodriguez-Lanetty M (2019) Proteomic basis of symbiosis: a heterologous partner fails to duplicate homologous colonization in a novel cnidarian– Symbiodiniaceae mutualism. Front Microbiol 10: 1153

Miura O, Keawtawee T, Sato N, Onodera K (2014) Vertical zonation of endosymbiotic zooxanthellae within a population of the intertidal sea anemone, *Anthopleura uchidai*. Mar Biol 161: 1745–1754

Nguyen LT, Schmidt HA, von Haeseler A, Minh BQ (2015) IQ-TREE: A fast and effective stochastic algorithm for estimating maximum-likelihood phylogenies. Mol Biol Evol 32: 268–274

Qian H, Chen W, Sun L, Jin Y, Liu W, Fu Z (2009) Inhibitory effects of paraquat on photosynthesis and the response to oxidative stress in *Chlorella vulgaris*. Ecotoxicol 18: 537–543

Sargent TD, Jamrich M, David IB (1986) Cell interactions and the control of gene activity during early development of *Xenopus laevis*. Dev Biol 114: 238–246

Schoenberg DA, Trench RK (1980) Genetic variation in *Symbiodinium* (= *Gymnodinium*) *microadriaticum* Freudenthal, and specificity in its symbiosis with marine invertebrates. III. Specificity and infectivity of *Symbiodinium microadriaticum*. Proc R Soc B 207: 445–460

Schwartz JA, Krupp DA, Weis VM (1999) Late larval development and onset of symbiosis in the Scleractinian coral *Fungia scutaria*. Biol Bull 196: 70–79

Wang JT, Meng PJ, Sampayo E, Tang SL, Chen CA (2011) Photosystem II breakdown induced by reactive oxygen species in freshly isolated *Symbiodinium* from *Montipora* (Scleractinia; Acroporidae). Mar Ecol Prog Ser 422: 51–62

Weis VM (2019) Cell biology of coral symbiosis: Foundational study can inform solutions to the coral reef crisis. Integr Comp Biol 59: 845–855

Weis VM, Davy SK, Hoegh-Guldberg O, Rodriguez-Lanetty M, Pringle JR (2008) Cell biology in model systems as the key to understanding corals. Trends Ecol Evol 23: 369–376

Wolfowicz I, Baumgarten S, Voss PA, Hambleton E, Voolstra CR, Hatta M, Guse A (2016) *Aiptasia* sp. larvae as a model to reveal mechanisms of symbiont selection in cnidarians. Sci Rep 6: 32366

Xiang T, Hambleton EA, DeNofrio JC, Pringle JR, Grossman AR, Lin S (2013) Isolation of clonal axenic strains of the symbiotic dinoflagellate *Symbiodinium* and their growth and host specificity. J Phycol 49: 447–458

Yamashita H, Suzuki G, Hayashibara T, Koike K (2013) *Acropora* recruits harbor ''rare'' *Symbiodinium* in the environmental pool. Coral Reefs 32: 355–366

Yamashita H, Suzuki G, Kai S, Hayashibara T, Koike K (2014) Establishment of coral–algal symbiosis requires attraction and selection. PLOS ONE 9: e97003

Yanagi K, Daly M (2004) The hermaphroditic sea anemone *Anthopleura atodai* n. sp. (Anthozoa: Actiniaria: Actiniidae) from Japan, with a redescription of *A. hermaphroditica*. Proc Biol Soc Washington 117: 408–422

Yorifuji M, Harii S, Nakamura R, Fudo M (2017) Shift of symbiont communities in *Acropora tenuis* juveniles under heat stress. PeerJ 5: e4055

(Received November 8, 2022 / Accepted December 25, 2022 / Published online April 17, 2023)